Attractively bound pairs of atoms in the Bose-Hubbard model and antiferromagnetism

Bernd Schmidt, Michael Bortz, Sebastian Eggert, and Michael Fleischhauer

Department of Physics and Research Center OPTIMAS, University of Kaiserslautern, D-67663 Kaiserslautern, Germany

David Petrosyan

Institute of Electronic Structure and Laser, FORTH, 71110 Heraklion, Crete, Greece
(Received 27 February 2009; published 30 June 2009)

We consider a periodic lattice loaded with pairs of bosonic atoms tightly bound to each other via strong attractive on-site interaction that exceeds the intersite tunneling rate. An ensemble of such lattice dimers is accurately described by an effective Hamiltonian of hard-core bosons with strong nearest-neighbor repulsion, which is equivalent to the *XXZ* model with Ising-like anisotropy. We calculate the ground-state phase diagram for a one-dimensional system, which exhibits incompressible phases, corresponding to an empty and a fully filled lattice (ferromagnetic phases) and a half-filled alternating density crystal (antiferromagnetic phase), separated from each other by compressible phases. In a finite lattice the compressible phases show characteristic oscillatory modulations on top of the antiferromagnetic density profile and in density-density correlations. We derive a kink model that provides simple quantitative explanation of these features. To describe the long-range correlations of the system, we employ the Luttinger-liquid theory with the relevant Luttinger parameter K obtained exactly using the Bethe-ansatz solution. We calculate the density-density as well as first-order correlations and find excellent agreement with numerical results obtained with density-matrix renormalization-group methods.

I. INTRODUCTION

Various idealized models describing many-body quantum systems on a lattice, such as the Heisenberg spin and the Hubbard models, have been widely studied for decades in condensed-matter physics [1,2]. With the recent progress in cooling and trapping bosonic and fermionic atoms in optical lattices [3], some of these models can now be realized in the laboratory with unprecedented accuracy—the Hubbard model being a case in point [4]. Implementing more general models, e.g., extended Hubbard or asymmetric spin model, with atoms in optical lattice potentials is, however, more challenging but potentially very rewarding. The purpose of the present paper is to study an experimentally relevant situation realizing the extended Hubbard model or, equivalently, an antiferromagnetic (AFM) *XXZ* model in the Ising-like phase with cold neutral atoms in a deep optical lattice potential.

We consider an optical lattice realization of the Bose-Hubbard model with strong on-site attractive interaction between the atoms. Specifically, we study a situation when each site of the lattice is loaded with either zero or two atoms. Experimentally, this can be accomplished by adiabatically dissociating a pure sample of Feshbach molecules in a lattice with at most one molecule per site [5,6]. The on-site attractive interaction then results in the formation of attractively bound atom pairs [7,8]—"dimers"—whose repulsive analog was realized in a recent experiment [6].

For strong atom-atom interaction, either attraction or repulsion, the dimer constituents are well colocalized [8], and an ensemble of such dimers in a lattice can be accurately described by an effective Hamiltonian, which has the form of a spin-$\frac{1}{2}$ *XXZ* model with Ising-like anisotropy. The derivation of the effective Hamiltonian is given in [9], where we

have also discussed its properties for the case of repulsive atom-atom interactions. Since the resulting nearest-neighbor attraction of dimers dominates the kinetic energy, below a critical temperature the dimers form minimal surface "droplets" on a lattice. In the case of attractive atom-atom interaction considered here, the interaction between the nearest-neighbor dimers is a strong repulsion. We then find that the ground state of the system of dimers in a grand canonical ensemble exhibits incompressible phases, corresponding to an empty and a fully filled lattice as well as a half-filled alternating density "crystal." These phases are separated from each other by compressible phases.

We calculate numerically and analytically the ground-state phase diagram for this system in one dimension. The critical points can be obtained with the help of the Bethe-ansatz, making use of the correspondence to the *XXZ* model [10]. In a finite lattice and close to half filling, the compressible phases show characteristic oscillatory modulations on top of the antiferromagnetic density profile. A simple kink model is derived, which explains the density profiles as well as number-number correlations in the compressible phases. The long-range correlations of the dimer system show a Luttinger-liquid behavior. We calculate the amplitude and the density correlations in a finite system from a field theoretical model, which show excellent agreement with the numerical data. The corresponding Luttinger parameter is obtained by solving the Bethe integral equations. Finally, we briefly discuss the implications of tunable nearest-neighbor interactions, which could be realized with dimers consisting of two different atomic species.

II. EFFECTIVE DIMER MODEL

We consider attractively bound dimers on a d-dimensional isotropic lattice. Because of the strong on-site atom-atom

interaction $U < 0$, it is energetically impossible to break the dimers, which effectively play the role of hard-core bosons on the lattice. Via a second-order process in the original atom hopping $J \ll |U|$, the dimers can tunnel to neighboring sites with the rate $\tilde{J} \equiv -2J^2/U > 0$ and carry nearest-neighbor interaction fixed at $4\tilde{J}$. The effective Hamiltonian for the system has been derived in [9],

$$\hat{H}_{\text{eff}} = \sum_j (2\varepsilon_j + U - 2d\tilde{J})\hat{m}_j - \tilde{J}\sum_{\langle j,i\rangle} \hat{c}_j^\dagger \hat{c}_i + 4\tilde{J}\sum_{\langle j,i\rangle} \hat{m}_j\hat{m}_i, \quad (1)$$

where $\hat{c}_j^\dagger$ and $\hat{c}_j$ are the creation and the annihilation operators and $\hat{m}_j = \hat{c}_j^\dagger \hat{c}_j$ is the number operator for a dimer at site j. In the first term of Eq. (1), the local potential energy $2\varepsilon_j$ of the pair of atoms is modified by an additional "internal energy" of the dimer $(U - 2d\tilde{J})$, which is negative for attractive interactions, so that the effective local chemical potential is given by $\mu_j = |U| + 2d\tilde{J} - 2\varepsilon_j$. The kinetic energy of one dimer described by the second term of Eq. (1) spans the interval $[-2d\tilde{J}, 2d\tilde{J}]$ corresponding to a Bloch band of a d-dimensional square lattice. In comparison, bringing a pair of dimers to neighboring sites requires an energy of $8\tilde{J}$ due to the strong repulsive interaction in the last term.

Since the dimers are effectively hard-core bosons, we can map the above Hamiltonian onto a spin system using the well-known Holstein Primakoff transformation

$$\hat{S}_j^z = \hat{m}_j - 1/2,$$

$$\hat{S}_j^+ = \hat{c}_j^\dagger \sqrt{1 - \hat{m}_j},$$

$$\hat{S}_j^- = \sqrt{1 - \hat{m}_j}\,\hat{c}_j, \quad (2)$$

which preserves the SU(2) commutation relations exactly. Since double occupancy is forbidden, $m_j = 0$ or 1, the factor $\sqrt{1 - \hat{m}_j}$ is zero for an occupied site and unity for an empty site. Therefore, we simply have $\hat{S}_j^+ = \hat{c}_j^\dagger$ and $\hat{S}_j^- = \hat{c}_j$, so that the equivalent Hamiltonian is given by

$$\hat{H}_{\text{spin}}/2\tilde{J} = -\frac{1}{2}\sum_{\langle j,i\rangle} (\hat{S}_i^+\hat{S}_j^- - 4\hat{S}_i^z\hat{S}_j^z) + \sum_j h_j\hat{S}_j^z, \quad (3)$$

with an effective magnetic field $h_j = (\varepsilon_j + U/2)/\tilde{J} + 3d$. This is the antiferromagnetic *XXZ* spin model with a fixed anisotropy of 4, i.e., for $h = 0$, the model is in the gapped Ising-like phase. A given total number N of dimers in a lattice of N_s sites correspond, in the spin model, to a fixed total magnetization $M_z = N - \frac{1}{2}N_s$.

III. DIMER SYSTEM IN ONE DIMENSION

It is now clear that the behavior of the dimer system in one dimension can be determined via isomorphic mapping of Eq. (1) onto the one-dimensional (1D) integrable *XXZ* model in a uniform field,
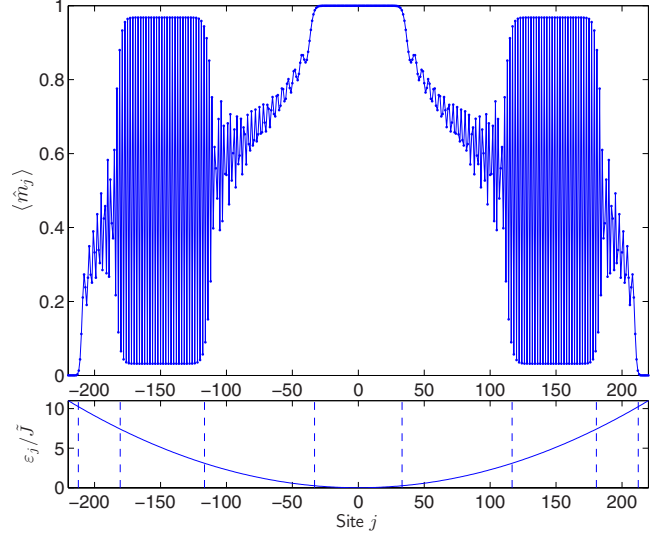

FIG. 1. (Color online) Density of dimers in a 1D lattice and weak harmonic potential obtained from DMRG simulation with $\mu_j = 18.5\tilde{J} - 2\varepsilon_j$ ($U/\tilde{J} = -16.5$) and $\varepsilon_j/\tilde{J} = j^2/4400$. One clearly identifies the incompressible phase with homogeneous filling of $\langle \hat{m}_j \rangle = 1$ in the trap center and two AFM phases, separated by compressible intermediate regions.

$$\hat{H}_{XXZ} = -\sum_{j=1}^{N_s-1} (\hat{S}_j^x\hat{S}_{j+1}^x + \hat{S}_j^y\hat{S}_{j+1}^y - \Delta\hat{S}_j^z\hat{S}_{j+1}^z) + h\sum_{j=1}^{N_s} \hat{S}_j^z, \quad (4)$$

where Δ is the anisotropy of the spin-spin interaction.

A. Ground-state phase diagram

An important general feature of the dimer model in Eq. (1) is that the ratio of interaction to kinetic energy has a fixed value larger than 1. As a consequence, the ground state of the system is dominated by interaction giving rise to interesting correlation properties.

In a homogeneous system, the ground state of the system depends only on a single parameter $\mu/\tilde{J}$. The corresponding phase diagram can be completely mapped out in an experiment by adding a shallow external trapping potential with sufficiently small confinement such that the local density approximation is valid and $\mu_j = |U| + 2\tilde{J} - 2\varepsilon_j$ does not change significantly over many lattice sites. Then different regions in the trap would correspond to different chemical potentials μ.

In Fig. 1 we plot the density of dimers in a one-dimensional lattice and an additional harmonic trapping potential obtained by numerical density-matrix renormalization-group (DMRG) calculations [11]. One clearly recognizes three types of regions: in the trap center, where the local chemical potential is largest, there is a unit filling of dimers. Separated by a spatial region of monotonously decreasing average filling follows a region where the average filling is exactly one half and the dimers form a periodic pattern with period 2 and almost maximum modulation depth. In this region, the dominant effect is the nearest-neighbor repulsion $4\tilde{J} > 0$ of Eq. (1). Toward the edge of the dimer cloud, the average density decreases again

monotonously to zero. In terms of the equivalent spin system, the central region corresponds to a gapped phase of full spin polarization imposed by a large negative effective magnetic field. The region of exactly one half average filling corresponds to another gapped phase with AFM order induced by the strong Ising-like interaction $-4\hat{S}_j^z\hat{S}_{j+1}^z$ of Eq. (3). The intermediate regions are compressible.

The critical values of the chemical potential for the transitions between compressible and incompressible phases in one dimension are known from the work of Yang and Yang [10] on the *XXZ* model of Eq. (4). For the parameters of the present system, we have

$$\mu_\downarrow/\widetilde{J} = -2, \tag{5a}$$

$$\mu_{\mathrm{AFM}-}/\widetilde{J} = 8 - 2\sqrt{15}\sum_{n=-\infty}^{\infty}\frac{(-1)^n}{\cosh[n\,\mathrm{arccosh}(4)]}$$

$$\approx 3.683\,61\ldots, \tag{5b}$$

$$\mu_{\mathrm{AFM}+}/\widetilde{J} = 8 + 2\sqrt{15}\sum_{n=-\infty}^{\infty}\frac{(-1)^n}{\cosh[n\,\mathrm{arccosh}(4)]}$$

$$\approx 12.316\,38\ldots, \tag{5c}$$

$$\mu_\uparrow/\widetilde{J} = 18. \tag{5d}$$

These values agree very well with those obtained from exact diagonalization on a small homogeneous lattice with $N_s = 10$ sites and periodic boundary conditions, as well as DMRG simulation with up to $N_s = 300$ and open boundary conditions. They also match the different regions of Fig. 1 as indicated by the vertical dashed lines in the lower part of the figure.

B. Mott-insulating phases

In the language of spin Hamiltonian, phases with zero ($N=0$) or full ($N=N_s$) filling correspond to ferromagnetic phases with a simple form of the ground state

$$|\psi_\downarrow\rangle = |\downarrow,\downarrow,\downarrow,\ldots,\downarrow\rangle, \tag{6}$$

$$|\psi_\uparrow\rangle = |\uparrow,\uparrow,\uparrow,\ldots,\uparrow\rangle. \tag{7}$$

Particle-hole excitations are not possible in the insulating state (7), while inserting a particle into Eq. (6) or removing one from Eq. (7), corresponding to flipping a spin, carries finite energy cost given by Eqs. (5a) and (5d). Hence these phases are incompressible.

For half filling ($N=\frac{1}{2}N_s$) the situation corresponds most closely to an AFM phase. However, in this case the simple Néel state

$$|\psi_{\mathrm{AFM}}^{(0)}\rangle = |\ldots,\downarrow,\uparrow,\downarrow,\uparrow,\downarrow,\uparrow,\downarrow,\uparrow,\ldots\rangle \tag{8}$$

is not an exact eigenstate of the full Hamiltonian $\hat{H}_{\mathrm{eff}}$ in Eq. (1). Rather, $|\psi_{\mathrm{AFM}}^{(0)}\rangle$ is an eigenstate of Hamiltonian $\hat{H}_{\mathrm{eff}}^{(0)}$

$\equiv \hat{H}_{\mathrm{eff}} - \hat{H}_{\mathrm{hop}}$ without the hopping term $\hat{H}_{\mathrm{hop}} = -\widetilde{J}\Sigma_j(\hat{c}_{j+1}^\dagger\hat{c}_j + \hat{c}_j^\dagger\hat{c}_{j+1})$. Due to $\hat{H}_{\mathrm{hop}}$ a dimer can tunnel from an occupied site to a neighboring empty site, which in terms of the Néel state (8), corresponds to flipping two neighboring spins, resulting in a state of the form

$$|\psi_j^{(1)}\rangle = |\ldots,\downarrow,\uparrow,\downarrow,\downarrow_j,\uparrow_{j+1},\uparrow,\downarrow,\uparrow,\ldots\rangle. \tag{9}$$

If we assume periodic boundary conditions and an even number of lattice sites N_s, there are $j=1,\ldots,N_s$ different states (9), one for each link where two neighboring spins can be flipped. Each of those states $|\psi_j^{(1)}\rangle$ has a larger repulsive (Ising) interaction energy $E_j^{(1)}$, which is increased by $8\widetilde{J}$ relative to energy $E_{\mathrm{AFM}}^{(0)}$ of state $|\psi_{\mathrm{AFM}}^{(0)}\rangle$. It is tempting to treat the smaller hopping $\hat{H}_{\mathrm{hop}}$ as perturbation with respect to $\hat{H}_{\mathrm{eff}}^{(0)}$, but unfortunately already the first-order correction carries a contribution from all N_s possible states in Eq. (9). In higher-order perturbation theory the number of contributing states increases with higher powers in N_s, so that the perturbation series diverges in the thermodynamic limit.

However, if we are interested in local observables, such as the density in Fig. 1, we can restrict the perturbation to only those hopping terms that affect the density at a given point. In particular, in order to calculate the expectation value $\langle\psi_{\mathrm{AFM}}|S_j^z|\psi_{\mathrm{AFM}}\rangle$, we make the following ansatz for the ground state $|\psi_{\mathrm{AFM}}\rangle$:

$$|\psi_{\mathrm{AFM}}\rangle \approx |\psi_{\mathrm{AFM}}^{(0)}\rangle + \sum_{i=j-1}^{j}\frac{|\psi_i^{(1)}\rangle\langle\psi_i^{(1)}|\hat{H}_{\mathrm{hop}}|\psi_{\mathrm{AFM}}^{(0)}\rangle}{E_{\mathrm{AFM}}^{(0)} - E_i^{(1)}}$$

$$= |\psi_{\mathrm{AFM}}^{(0)}\rangle + \frac{1}{8}(|\psi_{j-1}^{(1)}\rangle + |\psi_j^{(1)}\rangle), \tag{10}$$

which can be normalized by a factor of $1/\sqrt{1+1/32}$. This state is in general a poor approximation to the ground state, but it describes very well which terms in the Hamiltonian affect the local density at site j, since higher-order hopping contributes only 1/64 or less. Accordingly, the local density is given by

$$\langle\psi_{\mathrm{AFM}}|S_j^z|\psi_{\mathrm{AFM}}\rangle \approx (-1)^j\frac{32}{66}\left(1-\frac{1}{32}\right) = (-1)^j\frac{31}{66}, \tag{11}$$

which corresponds to a deviation of about 0.03 from perfect alternating order. Our numerical results for homogeneous systems show a deviation of about 0.032, which is in very good agreement with the prediction. Even though the half-filling state always implicitly contains excitations of type (9), the removal or the addition of a particle still costs relatively large energy given by Eq. (5b) or Eq. (5c), which makes the AFM phase incompressible.

C. Properties of compressible phases

In the remainder of this section, we examine the compressible phases, mainly in the vicinity of the antiferromagnetic phase, using two different approaches. The first is perturbative in nature and relies on the fact that the nearest-neighbor interaction energy between the dimers exceeds the dimer hopping energy by a large factor of 8. We show that the system can approximately be treated as a noninteracting
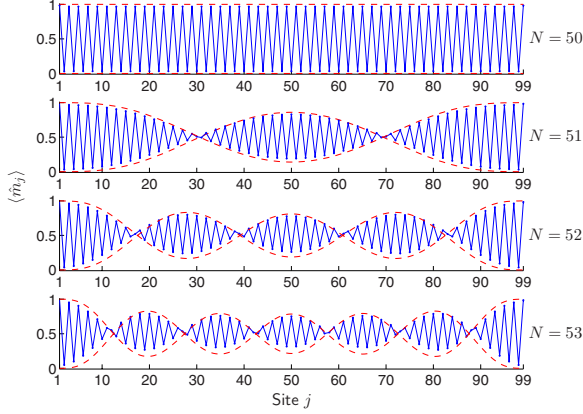
FIG. 2. (Color online) Particle density profile in a homogeneous lattice with $N_s = 99$ sites and hard-wall boundaries, for different particle numbers N. For half filling, $N = 50$, the ground state has nearly perfect AFM order. Adding one, two, and three particles leads to the density-wave modulations with the number of nodes equal twice the number of additional particles.

gas of kinks that behave like hard-core bosons. The second approach aims to describe long-range correlations employing the Luttinger-liquid theory. The relevant Luttinger parameter can be obtained by Bethe-ansatz solution of the equivalent *XXZ* spin model.

1. Noninteracting kink approximation

In Fig. 2 we plot the density distribution of dimers in a homogeneous lattice of $N_s = 99$ sites obtained from DMRG simulations with different numbers of dimers N. An infinite (hard-wall) confining potential $\varepsilon_0 = \varepsilon_{100} \rightarrow +\infty$ has been used, which imposes on Hamiltonian (1) open boundary conditions with $m_0 = m_{100} = 0$. Due to the asymmetric coupling at the boundaries, the end sites $j = 1$ and $j = 99$ prefer to be occupied with a particle. To accommodate an oscillating density wave, we therefore take odd number of lattice sites N_s. Note that the open boundary condition for the particles in Eq. (1) corresponds to an additional effective edge field $h_1 = h_{99} = -2$ for the spins in the *XXZ* model of Eq. (3), which has the analogous effect of polarizing both end spins up.

As seen in Fig. 2, the ground state for $N = 50$ exhibits density oscillations corresponding to the AFM Néel order, up to the small correction discussed in Sec. III B. Adding particles leads to modulated density distribution, with the envelope of modulation having regularly spaced nodes whose number is equal to twice the number of additional particles. In the following we will provide a simple theoretical understanding for this effect.

Without the small hopping term $\hat{H}_{hop}$, the ground state of Hamiltonian (1) for half filling is the AFM state $|\psi_{AFM}^{(0)}\rangle$ of Eq. (8), which is twofold degenerate. The AFM order with period 2 effectively doubles the size of the unit cell. Adding then a particle to $|\psi_{AFM}^{(0)}\rangle$ costs exactly an energy of $(h+8)\tilde{J}$, resulting in state

$$|\ldots,\uparrow,\downarrow,\uparrow_j,\uparrow_{j+1},\uparrow,\downarrow,\uparrow,\downarrow,\uparrow,\ldots\rangle,$$

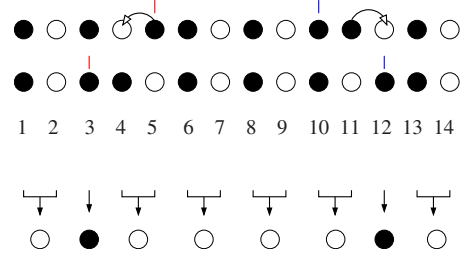which is energy degenerate with any state of the form

FIG. 3. (Color online) Top: 1D chain with one particle added to the AFM state creating a pair of odd (red; site 5) and even (blue; site 10) kinks. The hopping Hamiltonian $\hat{H}_{hop}$ leads to a motion of the odd and the even kinks on odd or even site, respectively. Interchange of odd- and even-site kinks is not possible. Bottom: mapping onto an effective lattice with a lattice constant of 2.

$$|\psi_{AFM+1}^{(0)}\rangle = |\ldots,\uparrow,\downarrow,\uparrow_j,\uparrow,\downarrow, \ldots ,\downarrow,\uparrow_{j'},\uparrow,\downarrow,\ldots\rangle. \quad (12)$$

Hence, the additional particle causes effective domain walls, which can be placed anywhere in the system and play the role of mobile kinks at positions j and j' between AFM regions with different orientations. Note that without hopping any number of particles above half filling can be created at the critical field $h_c^{(-)} = -8$ and placed in an arbitrary arrangement as long as no two neighboring lattice sites are empty. In other words, at $h_c^{(-)}$ we have a huge degeneracy of states with any magnetization $M_z \geq 0$, corresponding to arbitrary arrangement of antiferromagnetic regions and spin-up ferromagnetic regions. The analogous statement is also true at the upper critical field $h_c^{(+)} = 8$, where the degenerate subspace is defined as states with $M_z \leq 0$ where no two neighboring spins may point up. This degeneracy implies that without hopping the transition from the antiferromagnetic incompressible phase to the ferromagnetic incompressible phases is infinitely sharp at the effective critical magnetic fields $h_c^{(\pm)}$. As we will see below, however, the hopping lifts this degeneracy and is therefore crucial for the stability of compressible phases over finite ranges of field h as observed in Fig. 1.

The hopping $\hat{H}_{hop}$ is also responsible for the modulated wave patterns seen in Fig. 2. Starting from the AFM state in Eq. (8), we now insert more and more particles, each producing a pair of kinks. The states in Eq. (12) can be considered as AFM states with a pair of kinks, one at even sites and one at odd sites, e.g., state $|\downarrow_1,\uparrow_2,\downarrow_3,\uparrow_4,\uparrow_5,\uparrow_6,\downarrow_7,\uparrow_8,\downarrow_9,\ldots\rangle$ has kinks at sites 4 and 5, while state $|\downarrow_1,\uparrow_2,\downarrow_3,\uparrow_4,\uparrow_5,\downarrow_6,\uparrow_7,\uparrow_8,\downarrow_9,\ldots\rangle$ has kinks at sites 4 and 7. $\hat{H}_{hop}$ has nonvanishing matrix elements within the subspace of energy degenerate states with fixed number of additional particles. Within this manifold of states, hopping of the additional particle corresponds to free motion of kinks, wherein an even-site kink moves only on even sites and an odd-site kink on odd sites, as illustrated in the top part of Fig. 3. Furthermore, the even- and odd-site chain kinks cannot exchange their relative order. Note that hopping of a particle surrounded by two empty sites is energetically suppressed.

Given a fixed number of additional particles or holes, the motion of the corresponding kinks is equivalent to the mo-

tion of hard-core bosons in an effective lattice with lattice constant 2. To see this, consider the case of q additional particles on top of the half-filled lattice; the opposite case of holes follows from the particle-hole symmetry. Let the positions of the kinks be $j_1 < j_2 < \ldots < j_{2q}$. If j_1 is even (odd) then $j_3, j_5, j_7, \ldots$ are also even (odd) and $j_2, j_4, j_6, \ldots$ are odd (even). We now perform a mapping onto a new lattice which we call the kink lattice. The quasiposition k_n of the nth kink is then

$$k_n = \begin{cases} \dfrac{j_n + n - 1}{2} & \text{if } j_1 \text{ is even} \\[2mm] \dfrac{j_n + n}{2} & \text{if } j_1 \text{ is odd.} \end{cases} \qquad (13)$$

This mapping is illustrated in the lower part of Fig. 3.

Evaluating the matrix elements of the hopping Hamiltonian $\hat{H}_{\text{hop}}$ in the subspace of states with constant number of kinks, we find that the latter can be treated as hard-core bosons or noninteracting fermions on the kink lattice. The corresponding hopping strength on the period-2 lattice is again $\tilde{J}$. The exchange symmetry cannot be determined straightforwardly, and therefore we employ this approximation only to determine the density distribution of dimers. For simplicity, we choose the fermionic exchange symmetry.

Assuming a large lattice, we consider particle filling close to the antiferromagnetic case. In this limit, the kinks can be regarded as moving on a continuum. This means that the dynamics of the kinks can now be determined by solving the Schrödinger equation for noninteracting fermions. For $N = \frac{1}{2}N_s + 1$, i.e., one additional particle, we have a pair of kinks whose ground-state wave function is

$$\Psi_2(x_1, x_2) = \frac{\sqrt{2}}{L}\left[\sin\frac{\pi x_1}{L}\sin\frac{2\pi x_2}{L} - \sin\frac{\pi x_2}{L}\sin\frac{2\pi x_1}{L}\right], \qquad (14)$$

where $L = \frac{1}{2}N_s + 1$ is the length of the kink lattice. The leftmost kink shall move on the odd sites. A particle is sitting on an even site j if and only if one chain kink is to the left of j. Thus the density of particles on the even sites is

$$\langle \hat{m}(x) \rangle = 2\int_0^x dy_1 \int_x^L dy_2\, \Psi_2^*(y_1, y_2)\Psi_2(y_1, y_2). \qquad (15)$$

The prefactor of 2 emerges here because the integral occurs twice with interchanging the roles of y_1 and y_2. Although straightforward, we do not give the analytical expression of Eq. (15) since it is rather cumbersome. At the odd sites we get accordingly

$$1 - \langle \hat{m}(x) \rangle = \int_0^x dy_1 \int_0^x dy_2\, \Psi_2^*(y_1, y_2)\Psi_2(y_1, y_2)$$
$$+ \int_x^L dy_1 \int_x^L dy_2\, \Psi_2^*(y_1, y_2)\Psi_2(y_1, y_2). \qquad (16)$$

With q additional particles, the fermionic ground-state wave function for $2q$ kinks is

$$\Psi_{2q}(x_1, \ldots, x_{2q}) = \sum_P \frac{\text{sgn}(P)}{\sqrt{(2q)!}}\prod_{n=1}^{2q}\phi_{P(n)}(x_n), \qquad (17)$$

where the sum is over all permutations P of numbers $\{1, 2, 3, \ldots, 2q\}$ and

$$\phi_n(x) = \sqrt{\frac{2}{L}}\sin\frac{n\pi x}{L},$$

with $L = \frac{1}{2}N_s + q$. This results in the density distribution

$$\langle \hat{m}(x) \rangle = \sum_{k=0}^{q-1}\sum_{P,Q}\left[\frac{\text{sgn}(P)\text{sgn}(Q)}{(2k+1)\,!\,(2q-2k-1)!}\right.$$
$$\left.\times \prod_{n=1}^{2k+1} I(0, x, P(n), Q(n))\prod_{n=2k+2}^{2q} I(x, L, P(n), Q(n))\right], \qquad (18)$$

where Q denotes the permutations of $\{1, 2, 3, \ldots, 2q\}$, and

$$I(a, b, n, m) = \int_a^b dx\, \phi_n^*(x)\phi_m(x),$$

with $n, m \in \{1, 2, 3, \ldots, 2q\}$. In Eq. (18) we have taken into account that there are $\frac{(2q)!}{(2q-2k-1)!(2k+1)!}$ possibilities of choosing $2k+1$ kinks to the left of j.

The dashed red lines in Fig. 2 show the analytical results for the particle density in a box potential with the lattice filling slightly above one half obtained from the kink approximation. The agreement with the numerical DMRG data is rather good. The kink model also explains in a very intuitive way the pairwise appearance of nodes with adding every particle to the lattice.

Particle number correlations can be derived in the same manner. For two even sites at positions j_1 and j_2, the configurations contributing to the correlations correspond to an odd number of particles to the left of j_1, an even number of particles between j_1 and j_2, and an even number of particles to the right of j_2. The particle density-density correlations are then given by

$$\langle \hat{m}(x)\hat{m}(y) \rangle = \sum_{\substack{k_1,k_2,k_3=0 \\ \leq (q-1)}}^{k_1+k_2+k_3} \sum_{P,Q} \left[\frac{\text{sgn}(P)\text{sgn}(Q)}{(2k_1+1)\,!\,(2k_2)\,!\,(2k_3+1)!} \prod_{n=1}^{2k_1+1} I(0,x,P(n),Q(n)) \prod_{n=2k_1+2}^{2k_1+2k_2+1} I(x,y,P(n),Q(n)) \right.$$
$$\left. \times \prod_{n=2k_1+2k_2+2}^{2q} I(y,L,P(n),Q(n)) \right] \quad \text{for } x < y. \tag{19}$$

In Fig. 4 we plot the density-density correlations obtained from DMRG calculations (blue solid line) and the kink model (dashed red lines), displaying very good agreement. We finally note that within the approximation of non interacting kinks, first-order correlations exist only between neighboring sites. This perturbative model therefore cannot accurately describe such correlations.

2. Field theoretical approach

The spin chain equivalent to the dimer Hamiltonian (1) in one dimension is given by Eq. (4) with $\Delta=4$ and open boundary conditions. At zero magnetization $M_z=0$, the *XXZ* model (4) is gapped since $\Delta > 1$. However, as described in Sec. III A, the gap can be closed by a field between the two critical values, $h_c^{(-)} < h < h_c^{(+)}$. In other words, the system is critical for any nonzero magnetization away from the fully magnetized case. In this regime, the leading low-energy effective theory is a Luttinger liquid with two parameters: the spin velocity v and the Luttinger parameter K. These are functions of the magnetization per site $s^z = M_z/N_s$ and anisotropy Δ [12] (which for the particular dimer model here is fixed, $\Delta=4$). The Luttinger liquid is a free bosonic theory, which captures linear gapless low-energy scattering processes in momentum space above the ground state. Note that this free field theory is different from the noninteracting kink approximation of Sec. III C 1, where new quasiparticles—

which are approximately free in the dilute limit—were defined in direct space above the gapped ground state.

In order to calculate correlation functions, we first derive the Luttinger parameter $K(s^z)$ from the exact solution [13]. We write

$$K = \xi^2(b), \tag{20}$$

where the function $\xi(x)$ is determined by the integral equation

$$\xi(x) = 1 + \int_{-b}^{b} \kappa(x-y)\xi(y)dy, \tag{21}$$

with the kernel

$$\kappa(x) = \frac{1}{\pi} \frac{\sinh 2\eta}{\cos 2x - \cosh 2\eta}, \quad \Delta = \cosh \eta > 1.$$

The parameter b in Eqs. (20) and (21) is implicitly defined through

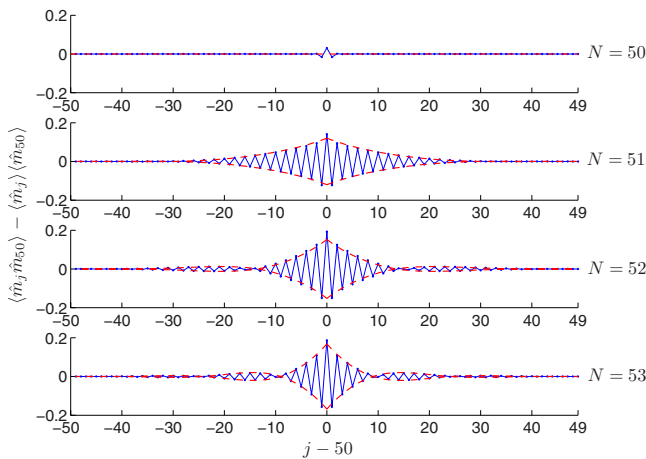$$s^z = \frac{1}{2} - \int_{-b}^{b} \rho(x)dx, \tag{22a}$$

FIG. 4. (Color online) Particle density-density correlations in a homogeneous lattice with $N_s=99$ sites and hard-wall boundaries, for different particle numbers N. The blue solid lines correspond to numerical DMRG results, while the red dashed lines correspond to the predictions of the kink approximation.
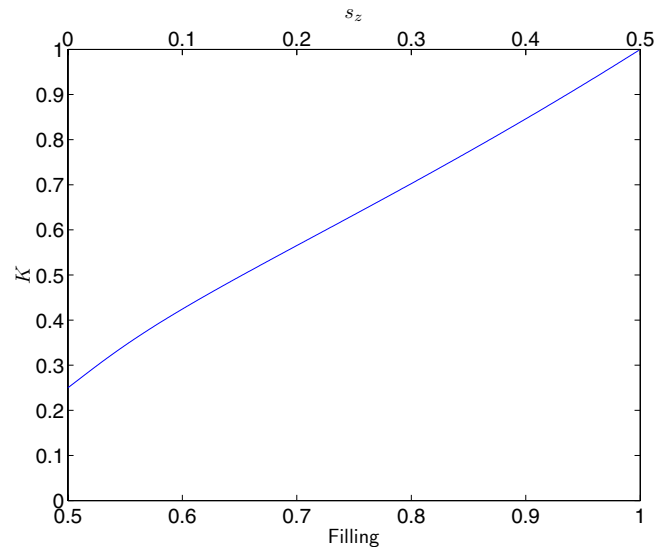

FIG. 5. (Color online) Dependence of the Luttinger parameter K on the mean lattice filling N/N_s, for $\Delta=4$.

$$\rho(x) = d(x) + \int_{-b}^{b} \kappa(x-y)\rho(y)dy, \tag{22b}$$

where

$$d(x) = \frac{1}{\pi} \frac{\sinh \eta}{\cos 2x - \cosh \eta}, \quad \Delta = \cosh \eta > 1.$$

Equations (20), (21), (22a), and (22b) are solved numerically by discretizing the integral and inverting the resulting matrix equation. Figure 5 shows the function $K(s^z)$ for $\Delta = 4$.

Within the Luttinger-liquid approach, one- and two-point correlation functions can be calculated using the standard mode expansion of bosonic fields [14] for open boundary conditions [15,16]. Then the spin-spin correlation function in the ground state reads

$$\langle \hat{S}^z(x)\hat{S}^z(y) \rangle = (s^z)^2 - B \frac{K}{8(N_s+1)^2} \left(\frac{1}{\sin^2 \frac{\pi(x-y)}{2(N_s+1)}} + \frac{1}{\sin^2 \frac{\pi(x+y)}{2(N_s+1)}} \right)$$
$$+ C_1 \frac{\cos[(2k_F + \theta/N_s)x + \varphi_1]}{\left(\sin \frac{\pi x}{N_s+1} \right)^K}$$
$$+ C_2 \frac{\cos[(2k_F + \theta/N_s)y + \varphi_2]}{\left(\sin \frac{\pi y}{N_s+1} \right)^K}$$
$$+ D \frac{\cos[(2k_F + \theta/N_s)x + \delta]}{\left(\sin \frac{\pi x}{N_s+1} \sin \frac{\pi y}{N_s+1} \right)^K} \left[\frac{\sin \frac{\pi(x+y)}{2(N_s+1)}}{\sin \frac{\pi(x-y)}{2(N_s+1)}} \right]^{2K}, \tag{23}$$

with the Fermi wave vector $k_F \equiv \pi(1-2s^z)/2$. Here the amplitudes $B, C_{1,2}, D$, the shift θ, and the phases $\varphi_{1,2}, \delta$ result from the bosonization of operators on the lattice. We con-
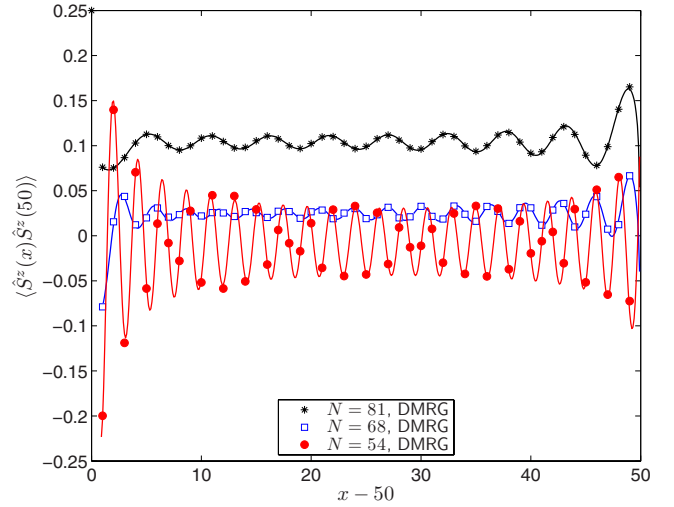

FIG. 6. (Color online) $\langle \hat{S}^z(x)\hat{S}^z(50) \rangle$ correlations obtained from the DMRG (dots) and the Luttinger-liquid approximation (solid lines).

sider them as parameters in Eq. (23) that are fixed numerically by fitting to the DMRG data. The exponents, however, are obtained from the Luttinger-liquid parameter K, which is given by the Bethe ansatz. Figure 6 shows the remarkable agreement between the two approaches. Note the shift in the wave vectors of the oscillations by a constant θ that depends on the boundary conditions, the interaction, and the magnetization. It has also been observed in the context of density oscillations in the open Hubbard model [17,18].

The corresponding result for the first-order correlation function in the ground state is

$$\langle \hat{S}^+(x)\hat{S}^-(y) \rangle = \left[\frac{\sqrt{\sin \frac{\pi x}{N_s+1} \sin \frac{\pi y}{N_s+1}}}{\sin \frac{\pi(x+y)}{2(N_s+1)} \sin \frac{\pi(x-y)}{2(N_s+1)}} \right]^{1/(2K)} \left(B \frac{\cos[(2k_F + \theta/N_s)(x-y) + \delta]}{\left(\sin \frac{\pi x}{N_s+1} \sin \frac{\pi y}{N_s+1} \right)^K} \left[\frac{\sin \frac{\pi(x+y)}{2(N_s+1)}}{\sin \frac{\pi(x-y)}{2(N_s+1)}} \right]^{2K} + C_1 \frac{\cos[(2k_F + \theta/N_s)x + \varphi_1]}{\left(\sin \frac{\pi x}{N_s+1} \right)^K} \right.$$
$$\left. + C_2 \frac{\cos[(2k_F + \theta/N_s)y + \varphi_2]}{\left(\sin \frac{\pi y}{N_s+1} \right)^K} \right). \tag{24}$$

Similarly to Eq. (23), the quantities $B, C_{1,2}, D, \delta, \phi_{1,2}, \theta$ are considered as fitting parameters. The resulting curves are shown in Fig. 7.

IV. ROLE OF ANISOTROPY Δ

The effective Hamiltonian (1) has a fixed ratio of the nearest-neighbor interaction to hopping, which results in a fixed Ising-like anisotropy $\Delta = 4$ in Eq. (3). It is interesting to also consider the more general case of tunable anisotropy. Such a scenario could, for example, be implemented with dimers consisting of two different atomic species with tun-

able interspecies interactions [19,20], as described below.

We thus consider two kinds of bosonic atoms, 1 and 2, in a tight-binding lattice realizing a two-species Hubbard model. Let J_1 and J_2 be the hopping rates and U_{11} and U_{22} be the on-site interaction strengths of the atoms of species 1 and 2, respectively, while U_{12} denote the interspecies on-site interaction. When $|U_{12}| \gg J_{1,2}$, a pair of atoms 1 and 2 localized on the same lattice site will form a tightly bound dimer [21]. We assume that each lattice site is initially populated with at most one dimer. In order to ensure that the dimers are stable, i.e., they will not dissociate upon collisions with each other, we impose additional conditions $|U_{11}| \gg J_1$ and $|U_{22}| \gg J_2$.
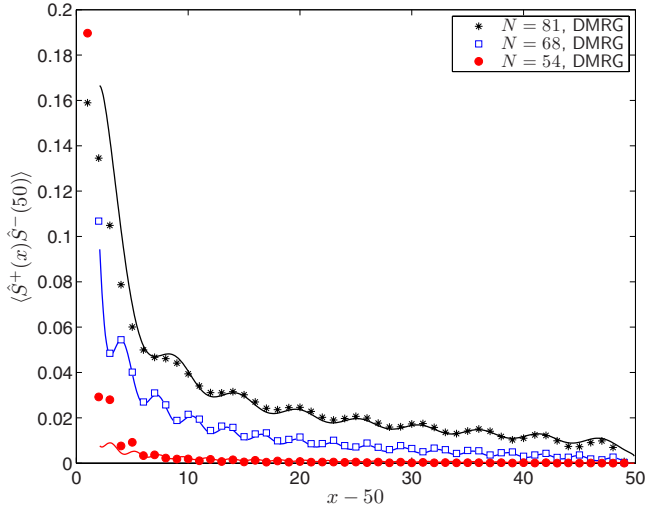
FIG. 7. (Color online) $\langle \hat{S}^+(x)\hat{S}^-(50)\rangle$ correlations obtained from the DMRG (dots) and the Luttinger-liquid approximation (solid lines).
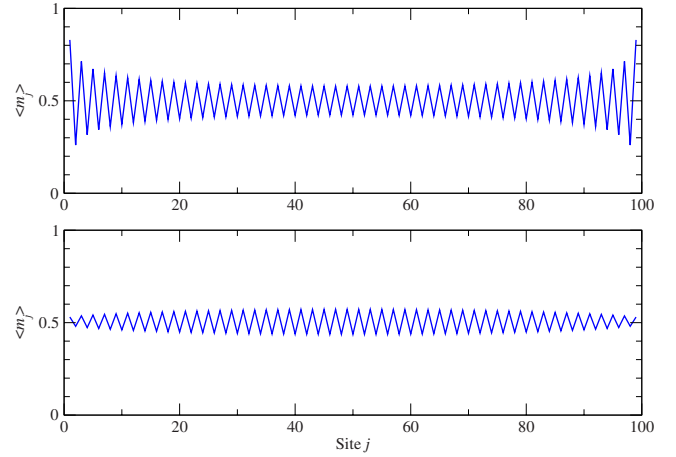

FIG. 8. (Color online) Top: ground-state density profile in a homogeneous lattice with $N_s=99$ sites and hard-wall boundaries, for $N=50$ particles, but with hopping strength equal to the nearest-neighbor repulsion, $\Delta=1$ (compare to Fig. 2, top panel). Bottom: the same, but without the effective edge fields in the spin chain model.

Following the procedure of Ref. [9], we use the second-order perturbation theory to adiabatically eliminate all the nonresonant states corresponding to unpaired atoms on neighboring lattice sites. The resulting effective Hamiltonian for the dimers is given by

$$\hat{H}_{\text{eff}} = -\widetilde{J}\sum_{\langle j,i\rangle} \hat{c}_j^\dagger \hat{c}_i + V\sum_{\langle j,i\rangle} \hat{m}_j \hat{m}_i - \sum_j \mu_j \hat{m}_j, \qquad (25)$$

where

$$\widetilde{J} \equiv -\frac{2J_1 J_2}{U_{12}},$$

$$V \equiv -\left(\frac{2J_1^2}{U_{11}} + \frac{2J_2^2}{U_{22}} + \frac{J_1^2 + J_2^2}{U_{12}}\right),$$

$$\mu_j \equiv -\left(\varepsilon_{1;j} + \varepsilon_{2;j} + U_{12} + 2d\frac{J_1^2 + J_2^2}{U_{12}}\right)$$

are, respectively, the dimer hopping rate, the nearest-neighbor interaction, and the effective local chemical potential with $\varepsilon_{1;j}$ ($\varepsilon_{2;j}$) being the potential energy of atom 1 (2) at site j. It is important to note that the dimers described by the above Hamiltonian behave as hard-core bosons, provided $|U_{11}+U_{22}+2U_{12}| \gg \widetilde{J}$. Yet, the dimer hopping rate $\widetilde{J}$ and the nearest-neighbor interaction V can be independently tuned by varying U_{11}, U_{22}, and/or U_{12} in the vicinity of Feshbach resonances [19,20]. One can thus tune the anisotropy parameter $\Delta = -V/\widetilde{J}$.

As the anisotropy becomes smaller, the perturbative analysis used in the previous sections becomes unreliable. It is known that the 1D model of Eq. (4) is critical for $-1 \leq \Delta \leq 1$. Therefore, the perturbation treatment breaks down exactly at the point where the hopping becomes equal to or

larger than the nearest-neighbor dimer-dimer interaction. However, it is still possible to use the field theoretical methods of Sec. III C 2 to calculate the correlation functions and the expectation values.

In the critical region excitations are gapless in the thermodynamic limit, so that there is no incompressible phase at half filling. The crossover between the completely filled and the completely empty regions in Fig. 1 is therefore continuous as a function of the effective field and there is no extended half-filled phase. The strength of hopping is therefore crucial for the behavior of the system: weak hopping enables the presence of a compressible phase between the incompressible ferromagnetic and antiferromagnetic phases. With increasing the hopping strength, the incompressible antiferromagnetic phase shrinks and completely vanishes when the hopping reaches the value of the nearest-neighbor interaction, $\Delta \leq 1$.

Equally interesting is the effect of hopping on the density of dimers along the chain. As discussed in Sec. III C, density-wave modulations appear in Fig. 2 because of the effective motion of kinks. The complex interplay between the kinetic and the interaction terms in the critical region now leads to further modification of the density pattern along the chain [22–24]. In particular, the amplitude of the ground-state density oscillations is now significantly reduced toward the middle of the chain with a characteristic dropoff as shown in Fig. 8. Excited states with larger N would then exhibit modulations on top of this ground-state pattern, similar to Fig. 2.

Interestingly, the exact form of the boundary conditions plays now a much more important role. Namely, the effective edge field of the spin chain model discussed in Sec III C 1 accounts for a large part of the ground-state density oscillations. For comparison, in Fig. 8 we also show the density for the spin chain model without any edge field. The density amplitude is now smaller near the boundary. At $\Delta=1$, this amplitude has been predicted to follow approximately a

$\sqrt{\sin(\pi x/N_s)}$ behavior [22], which however is strongly affected by temperature [23,24] due to the gapless modes.

V. SUMMARY

In this paper, we have studied the many-body dynamics of attractively bound pairs of atoms in the Bose-Hubbard model. When the on-site interaction between the atoms exceeds by a sufficient amount the bandwidth of the lowest single-particle Bloch band, the pairs are well colocalized and can be treated as composite dimer particles. Then the effective model for dimers on a lattice is equivalent to an asymmetric spin-$\frac{1}{2}$ *XXZ* model in an external magnetic field: the nearest-neighbor interaction between the dimers translates into an Ising-like spin-spin interaction and the dimer tunneling to a spin-spin coupling in the *x-y* plane.

The case of repulsively bound pairs studied in [9] corresponds to a ferromagnetic Ising coupling. In contrast, for attractively bound pairs analyzed here, the Ising coupling is antiferromagnetic leading to a much richer phase diagram. The asymmetry parameter Δ of the *XXZ* model is equal to 4; as a result, the system is gapped for both zero and full magnetizations. The zero magnetization state, corresponding to exactly half filling of dimers, exhibits antiferromagnetic order, while the full magnetization (ferromagnetic) states correspond to vanishing or full filling of dimers. When the effective magnetic field, or for that matter the chemical potential for the dimers, exceeds critical values, the gap is closed and the dimer system becomes critical with finite compressibility.

We have derived the critical values of the chemical potential for the transition points from the gapped ferromagnetic and antiferromagnetic phases to the compressible phases in one dimension, employing the known exact solutions of the *XXZ* model. Close to half filling, the system can be well described by kinklike domain walls that separate antiferromagnetic strings of opposite phase and can propagate through the lattice almost freely. A simple approximate description in terms of noninteracting kinks gives rather accurate predictions for the dimer density as well as nonlocal density-density correlations.

In order to explain the first-order correlations, we employed a field theoretical approach based on the Luttinger-liquid theory. The corresponding Luttinger parameter was obtained by solving the Bethe-ansatz equations for the equivalent *XXZ* model in the regime of critical magnetic fields. The expressions for the first-order and the density-density correlations showed remarkably good agreement with the numerical data obtained by DMRG simulations. Finally we discussed the consequences of changing the anisotropy parameter of the *XXZ* model, which could be realized with dimers consisting of two different atomic species. Our studies attest that interaction-bound pairs of atoms in deep optical lattices can provide a versatile tool to simulate and explore quantum spin models.

ACKNOWLEDGMENTS

[1] F. H. L. Essler, H. Frahm, F. Göhmann, A. Klümper, and V. E. Korepin, *The One-Dimensional Hubbard Model* (Cambridge University Press, Cambridge, 2008).

[2] R. Micnas, J. Ranninger, and S. Robaszkiewicz, Rev. Mod. Phys. **62**, 113 (1990).

[3] O. Morsch and M. Oberthaler, Rev. Mod. Phys. **78**, 179 (2006); I. Bloch, J. Dalibard, and W. Zwerger, *ibid.* **80**, 885 (2008); M. Lewenstein, A. Sanpera, V. Ahufinger, B. Damski, A. Sen De, and U. Sen, Adv. Phys. **56**, 243 (2007).

[4] D. Jaksch, C. Bruder, J. I. Cirac, C. W. Gardiner, and P. Zoller, Phys. Rev. Lett. **81**, 3108 (1998); M. Greiner, O. Mandel, T. Esslinger, T. W. Hänsch, and I. Bloch, Nature (London) **415**, 39 (2002); D. Jaksch and P. Zoller, Ann. Phys. (N.Y.) **315**, 52 (2005).

[5] G. Thalhammer, K. Winkler, F. Lang, S. Schmid, R. Grimm, and J. H. Denschlag, Phys. Rev. Lett. **96**, 050402 (2006); T. Volz, N. Syassen, D. M. Bauer, E. Hansis, S. Dürr, and G. Rempe, Nat. Phys. **2**, 692 (2006).

[6] K. Winkler, G. Thalhammer, F. Lang, R. Grimm, J. Hecker Denschlag, A. J. Daley, A. Kantian, H. P. Büchler, and P. Zoller, Nature (London) **441**, 853 (2006); J. Hecker Denschlag and A. J. Daley, in *Exotic Atom Pairs: Repulsively Bound States in an Optical Lattice*, Proceedings of the International School of Physics "Enrico Fermi," Course CLXIV on Ultra-

Cold Fermi Gases, edited by M. Inguiscio, W. Ketterle, and C. Salomon (IOS Press, Amsterdam, 2008).

[7] R. Piil and K. Mølmer, Phys. Rev. A **76**, 023607 (2007); N. Nygaard, R. Piil, and K. Mølmer, *ibid.* **78**, 023617 (2008).

[8] M. Valiente and D. Petrosyan, J. Phys. B **41**, 161002 (2008).

[9] D. Petrosyan, B. Schmidt, J. R. Anglin, and M. Fleischhauer, Phys. Rev. A **76**, 033606 (2007); **77**, 039908(E) (2008).

[10] C. N. Yang and C. P. Yang, Phys. Rev. **150**, 327 (1966).

[11] S. R. White, Phys. Rev. Lett. **69**, 2863 (1992); U. Schollwöck, Rev. Mod. Phys. **77**, 259 (2005).

[12] F. D. M. Haldane, Phys. Rev. Lett. **45**, 1358 (1980).

[13] N. M. Bogoliubov, A. G. Izergin, and V. E. Korepin, Nucl. Phys. B **275**, 687 (1986).

[14] For a review, see S. Eggert, in *Theoretical Survey of One Dimensional Wire Systems*, edited by Y. Kuk, S. Hasegawa, and Q. K. Xue (Sowha, Seoul, 2007), p. 13; e-print arXiv:0708.0003.

[15] S. Eggert and I. Affleck, Phys. Rev. B **46**, 10866 (1992).

[16] M. A. Cazalilla, J. Phys. B **37**, S1 (2004).

[17] G. Bedürftig, B. Brendel, H. Frahm, and R. M. Noack, Phys. Rev. B **58**, 10225 (1998).

[18] S. Söffing, M. Bortz, I. Schneider, A. Struck, M. Fleischhauer, and S. Eggert, Phys. Rev. B **79**, 195114 (2009).

[19] G. Thalhammer, G. Barontini, L. De Sarlo, J. Catani, F. Mi-

nardi, and M. Inguscio, Phys. Rev. Lett. **100**, 210402 (2008); J. Catani, L. De Sarlo, G. Barontini, F. Minardi, and M. Inguscio, Phys. Rev. A **77**, 011603(R) (2008).

[20] T. Best, S. Will, U. Schneider, L. Hackermuller, D. van Oosten, I. Bloch, and D.-S. Lühmann, Phys. Rev. Lett. **102**, 030408 (2009).

[21] R. T. Piil, N. Nygaard, and K. Mølmer, Phys. Rev. A **78**, 033611 (2008).

[22] S. Eggert, I. Affleck, and M. D. P. Horton, Phys. Rev. Lett. **89**, 047202 (2002); **90**, 089702 (2003).

[23] S. Eggert and I. Affleck, Phys. Rev. Lett. **75**, 934 (1995).

[24] S. Rommer and S. Eggert, Phys. Rev. B **62**, 4370 (2000).